Hindawi Publishing Corporation
International Journal of Photoenergy
Volume 2012, Article ID 149210, 7 pages
doi:10.1155/2012/149210

Research Article

Preparation and Characterization of $Cu(In,Ga)Se_2$ Thin Films by Selenization of $Cu_{0.8}Ga_{0.2}$ and In_2Se_3 Precursor Films

Jiang Liu, Da-Ming Zhuang, Ming-Jie Cao, Chen-Yue Wang, Min Xie, and Xiao-Long Li

Department of Mechanical Engineering, Tsinghua University, Beijing 100084, China

Correspondence should be addressed to Da-Ming Zhuang, dmzhuang@tsinghua.edu.cn

Received 1 August 2012; Accepted 31 October 2012

Academic Editor: Roel van De Krol

Se-containing precursor films with two different compositions were prepared by magnetron sputtering from $Cu_{0.8}Ga_{0.2}$ and In_2Se_3 targets, and then were selenized using Se vapor. The effects of precursor composition and selenization temperature on the film properties were investigated. The results show that $Cu_{2-x}Se$ phase plays a critical role in film growth and electrical properties of CIGS films. The Cu-rich films exhibit different surface morphology and better crystallinity, as compared to the Cu-poor films. All the CIGS films exhibit p-type conductivity. The resistivity of the Cu-rich films is about three orders of magnitude lower than that of the Cu-poor films, which is attributed to the presence of p-type highly conductive $Cu_{2-x}Se$ phase.

1. Introduction

$Cu(In_{1-x}Ga_x)Se_2$ (CIGS) thin films have received considerable attention in recent years because of their application in solar cells, which have many advantages in high conversion efficiency [1, 2], the possibility of low-cost production [3, 4], and long-term stability [5, 6]. The world-record efficiency for small-area CIGS-based thin film solar cells has recently surpassed 20% [7]. One of the special qualities of the CIGS material is its variable band-gap [8]. The bandgap of chalcopyrite CIGS absorber could vary from 1.04 eV in $CuInSe_2$ to 1.68 eV in $CuGaSe_2$ by substituting indium for gallium. The addition of small amounts of Ga could not only raise the bandgap to more suitably match the AM1.5 solar spectrum, more importantly, but could also improve the electrical properties of CIGS films [9–11]. However, the CIGS films with higher gallium concentration show a significant loss of efficiency relative to lower gallium content films [12]. The optimal [Ga]/[In + Ga] ratio of CIGS absorber for high efficiency CIGS solar cell is considered to be 0.2∼0.3 from a number of experimental results [13–15].

A variety of processing techniques have been developed to prepare high quality CIGS thin films. The two most reported processes are the coevaporation from elemental sources and the selenization of metallic precursors. The coevaporation process consists of three stages, which all need precise control over the deposition rate of each element. The selenization of metallic precursors is a two-stage process, which involves the deposition of Cu-In-Ga metallic precursors in the first step followed by their selenization using H_2Se gas or Se vapor [16]. The presence of low-melting metal indium in Cu-In-Ga metallic precursors could always result in rough morphologies of the CIGS films and loss of indium from films during the ramp-up and selenization stages [17, 18]. Moreover, the CIGS films by selenization of metallic precursors have a poor adhesion to substrate, due to a threefold volume expansion caused by the incorporation of Se into the metallic precursors during selenization [18]. Few works have been done using the selenium-containing precursors to prepare CIGS films. In this study, we introduce $Cu_{0.8}Ga_{0.2}$ and In_2Se_3 as precursor films and avoid the direct addition of elemental indium. The precursors were then treated by selenization using Se vapor. The effects of precursor compositions and selenization temperature on the film properties were investigated.

2. Experimental

High purity In_2Se_3 ceramic target and CuGa alloy target with Ga content of 20 at% were used. The size of the two targets is 360 mm × 80 mm. In the first step the CuGa and In_2Se_3

films were deposited on Mo-coated and bare soda-lime glass substrate by middle frequency (MF) magnetron sputtering of CuGa and In_2Se_3 targets. By adjusting the sputtering time and current of the two targets, the precursor films with different compositions could be prepared. Generally, relative proportion of metallic elements in CIGS films lies on that of the precursor films. The copper content of the final film and during the deposition process has a strong influence on film growth and CIGS solar cell properties [19, 20]. For the purpose of comparison, two sets of as-sputtered films were prepared. One was Cu-rich composition ([Cu]/[In + Ga] > 1) and another was Cu-poor composition ([Cu]/[In + Ga] < 1). The substrate holder inside the sputtering equipment could move back and forth along the short transverse direction of targets to keep the homogeneity of the as-sputtered films. The substrate temperature and working pressure during sputtering was kept constant at 200°C and 0.5 Pa, respectively. In the second step, the as-sputtered films were selenized with Se vapor in a three-chamber furnace which can be easily scaled up to provide a large-area in-line sequential CIGS process. Prior to heating, the chambers were evacuated and flushed two times with high purity nitrogen. The selenization time was held constant at 30 min and the selenization temperature varied from 400°C to 600°C.

Crystalline structures of the samples were examined by X-ray diffraction carried out with D/max-RB diffractometer (Rigaku) using Cu Ka radiation (0.1541 nm). The compositions of the films were tested by X-ray fluorescence (LAB CENTER XRF-1800). The surface and cross-section micrographs of the films were obtained by thermal field emission scanning electron microscope (TFE-SEM, LEO-1530). Raman spectra were recorded using Renishaw Raman microscope (model RM2000) with an argon ion laser wavelength of 514.5 nm. Hall-effect measurements were used on films grown on bare soda-lime glass to determine the resistivity and carrier concentration of CIGS films.

3. Results and Discussion

The XRD patterns of the precursor films deposited on bare soda-lime glass with two different compositions are presented in Figure 1. The corresponding composition data are shown in Table 1. To investigate the relative compositional change, the corresponding atomic ratios of Cu/(In + Ga), Ga/(In + Ga), and 2∗Se/(Cu+3∗(In + Ga)) were also calculated. The films were intentionally deposited into two groups, Cu-rich and Cu-poor precursor films, which have [Cu]/[In + Ga] of 1.277 and 0.935, respectively. Since Ga is incorporated in CuGa alloy target, the Cu-rich precursor film deserves to have a slightly higher [Ga]/[In + Ga] than the Cu-poor precursor film. The 2∗[Se]/([Cu]+3∗[In + Ga]) of the two precursor films are far less than that of near-stoichiometric $Cu(In_{1-x}Ga_x)Se_2$ compound and need be improved during selenization. Figure 1 indicates that XRD patterns of the two precursor films are almost the same. The diffraction peaks at $2\theta = 26.6°$ corresponds to (112) plane of CIGS chalcopyrite structure. Two broad peaks at around $2\theta = 44°$ are attributed to Cu (111) and CIGS (204/220). No In-Se

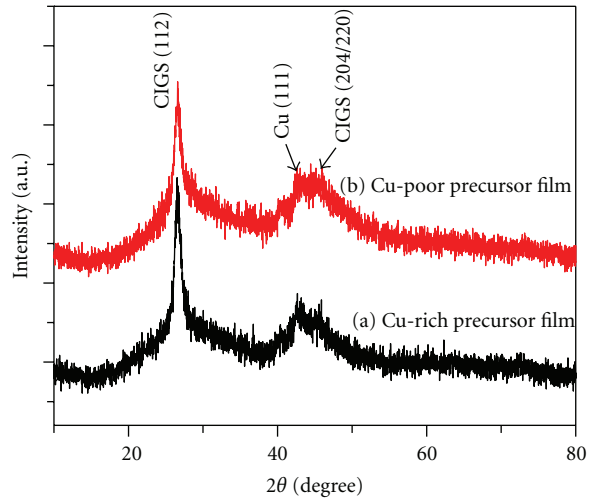

Figure 1: XRD patterns of the precursor films of two different compositions: (a) Cu-rich precursor film, (b) Cu-poor precursor film.

related peaks or other characteristic peaks are found, which could be explained by the low crystallinity of the films. After selenization at 550°C for 30 min, XRF measurements (Table 1) show that the CIGS films selenized from Cu-rich and Cu-poor precursor films still conserve their overall Cu-rich and Cu-poor compositions, respectively, with corresponding [Cu]/[In + Ga] of 1.293 and 0.938. The [Ga]/[In + Ga] ratios of the CIGS films are nearly equal to these of their respective precursor films, which could draw the conclusion that the element concentrations of indium and gallium kept almost constant during selenization. Additionally, the 2∗[Se]/([Cu]+3∗[In + Ga]) ratios improved noticeably after selenization, which of Cu-rich film is higher than that of Cu-poor film due to the monovalence chemical state of copper.

Figure 2 shows the XRD patterns of CIGS films selenized from Cu-rich precursor films at different selenization temperatures for 30 min. All samples show characteristic peaks of the chalcopyrite-type structure and are oriented along the (112) direction parallel to the substrate. The full width at half maximum (FWHM) of (112) peaks of the films decreases with the increase of selenization temperature, which may be attributed to the crystalline quality improvement and grain growth. For the CIGS film selenized at 550°C, two additional peaks at $2\theta = 31.4°$ and 55.9° could be found, which correspond to $MoSe_2$ (100) and $MoSe_2$ (110), respectively, according to Joint Committee on Powder Diffraction Standards (JCPDS) Number 29-0914. The intensity of the two peaks of $MoSe_2$ gets stronger when the selenization temperature increases from 550°C to 600°C, which is indicative of higher degree of selenization. Note that when the selenization temperature was 600°C, the soda-lime glass substrate warped but the film deposited on it still did not peel off and could be used for XRD analysis and other tests.

Figure 2(b) shows the detailed XRD patterns of CIGS films from $2\theta = 42°$ to 47° where (204/220) peak of chalcopyrite structure lies. Overall, the position of the (204/220) peak seems to shift to higher diffraction angle as

Table 1: Chemical compositions (measured by XRF) of the precursor films and subsequent selenized films at 550°C for 30 min.

Sample	Cu (at%)	In (at%)	Ga (at%)	Se (at%)	[Cu]/[In + Ga]	[Ga]/[In + Ga]	2∗[Se]/([Cu] + 3∗[In + Ga])
Cu-rich precursor film	39.80	21.87	9.29	29.05	1.277	0.298	0.436
Cu-poor precursor film	32.27	27.08	7.45	33.21	0.935	0.216	0.489
CIGS film selenized from Cu-rich precursor film	29.14	15.80	6.74	48.32	1.293	0.299	0.999
CIGS film selenized from Cu-poor precursor film	23.94	20.00	5.52	50.55	0.938	0.216	1.006

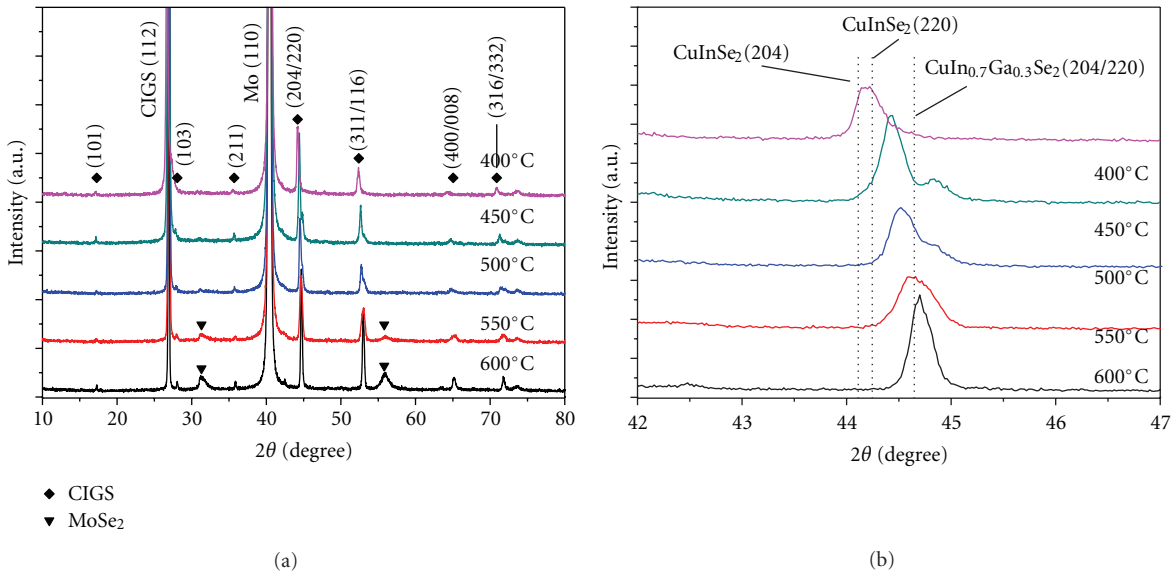

Figure 2: (a) XRD patterns of CIGS films selenized from Cu-rich precursor films at different selenization temperatures for 30 min. (b) Detailed XRD plots of the (204/220) peaks. JCPDS (Joint Committee on Powder Diffraction Standards) Numbers 42-1120, 29-0914, 40-1487, and 35-1102 are referred to for Mo, $MoSe_2$, $CuInSe_2$, and $CuIn_{0.7}Ga_{0.3}Se_2$, respectively.

the selenization temperature increases. The $Cu(In_{1-x}Ga_x)Se_2$ solid solution is based on $CuInSe_2$. Gallium is added to obtain CIGS with a wider bandgap; accordingly, the lattice constants, a and c, decrease. With the increasing of [Ga]/[In + Ga] ratio, the diffraction peaks of chalcopyrite phase shift to higher 2θ side. Theoretically, if the lattice constant c/a ratio does not equal two, the (204) and (220) peaks would uncouple. For the CIGS film selenized at 400°C, the splitting of the (204) and (220) peaks is observed, which is in very good agreement with the $CuInSe_2$ phase (JCPDS Number 40-1487). For the CIGS film selenized at 550°C or 600°C, the (204) and (220) peaks almost overlap, the positions of which match well with the $CuIn_{0.7}Ga_{0.3}Se_2$ solid solution (JCPDS Number 35-1102). Based on the above experimental observations, it could be concluded that $CuInSe_2$ may form first at a relatively low selenization temperature of 400°C, or the formation of $CuInSe_2$ occurs faster than the formation of $CuGaSe_2$, which is also observed in other literatures [21–23]. It could be easily understood that the selenization temperature has a strong influence on the reaction rate and atomic diffusion coefficient. With the increasing of selenization temperature, the gallium diffuses into $CuInSe_2$, thus resulting in the formation of $CuIn_{0.7}Ga_{0.3}Se_2$ solid solution.

To further investigate the structural properties of CIGS thin films, Raman spectroscopy was adopted. Raman spectra of CIGS films selenized at different selenization temperatures for 30 min from Cu-rich precursor films and Cu-poor precursor films are presented in Figure 3. All spectra are normalized to the peak at around 172–174 cm^{-1}, which corresponds to the dominant A_1 mode of CIGS films resulting from the vibration of the Se anions in the x-y plane with the cations at rest [24, 25]. And mixed B_2/E modes are also observed at around 213 cm^{-1}, which represent vibrations of anions and cations together [24]. For all the Cu-rich films (Figure 3(a)), an additional mode appears at around 258–260 cm^{-1}, which is assigned to the A_1 mode of Cu-Se compounds like CuSe or Cu_2Se and is labeled with $Cu_{2-x}Se$ in the following literatures [19, 26]. For the Cu-poor films (Figure 3(b)), the peak of $Cu_{2-x}Se$ A_1 mode exists only when the selenization temperature was 400°C. From the above observation, it is clear that inadequately reaction for the Cu-poor films at low selenization temperature could result in phase segregation. For the Cu-rich films, even at high selenization of up to 600°C, $Cu_{2-x}Se$ segregation is always present, which could be explained with the Cu_2Se-In_2Se_3 pseudo-binary phase diagram [27], where excess Cu couldn't be incorporated in the chalcopyrite phase.

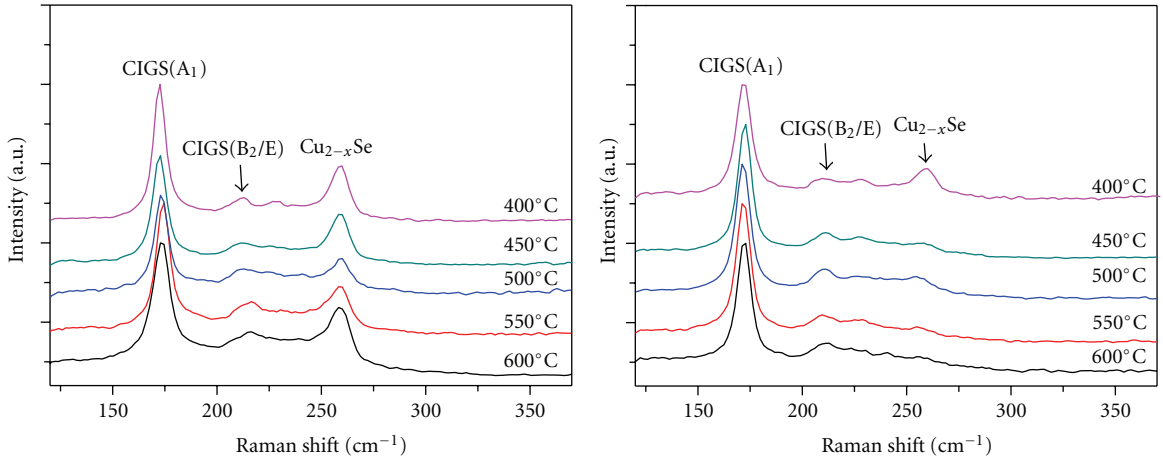

FIGURE 3: Raman spectra of CIGS films selenized at different selenization temperatures for 30 min from (a) Cu-rich precursor films, and (b) Cu-poor precursor films.

Surface SEM images of CIGS films selenized from Cu-rich precursor films and Cu-poor precursor films at different selenization temperatures are presented in Figure 4. The insets show the corresponding cross-section micrographs of the films. From Figure 4(a–e) and Figure 4(f–j), the crystallinity of the films improves noticeably as the selenization temperature increases. The Cu-rich films exhibit a granular surface morphology, whereas a triangular surface morphology is observed obviously for the Cu-poor films selenized at 550°C or 600°C. Low selenization temperature of 400°C results in a significant increase in surface roughness of the Cu-rich and Cu-poor films. In comparison with the Cu-poor films, the Cu-rich films have a larger grain size. When the selenization temperature was 500°C or above, the surface morphology of Cu-rich films exhibit closely packed grains which are approximate 1 μm wide. From the cross-section micrographs, the comparison of film growth between the Cu-rich films and the Cu-poor films is also evident. According to the growth model proposed by Klenk et al. [28], a low-temperature liquid Cu-Se phase is present for the Cu-rich films during selenization and can aid the film growth. Consequently, the difference of Cu content between two films could result in different morphology and grain size. Furthermore, the grain is layered along the cross-section direction, which is more obvious at relatively low selenization temperature. The grain size of the top layer is larger than that of the bottom layer. It could be explained with the degree of selenization. Higher selenization temperature could result in higher degree of selenization [29], which is also consistent with the XRD analysis. Since the reaction proceeds from the surface towards the bulk during selenization, the crystalline quality of the bottom layer increases as the selenization degree increases.

Figure 5 shows the resistivity and carrier concentration of CIGS films selenized from Cu-rich precursor films and Cu-poor precursor films as a function of selenization temperature. All the CIGS films exhibit p-type semiconductor material. In comparison with the Cu-poor films, a significant decrease in resistivity and increase in carrier concentration by several orders of magnitude are observed in the Cu-rich films, which can be explained by the electrical properties of p-type $Cu_{2-x}Se$ phase. The $Cu_{2-x}Se$ is a p-type highly conductive phase, could produce a large number of holes, and thus decreases the resistivity of bulk film. It should be noted that Cu-rich films with such high carrier concentration, which is beyond the optimum range of 10^{16}-10^{17} cm^{-3} [30], cannot be used for devices without further treatment. In both cases of the Cu-rich and Cu-poor films, the resistivity and carrier concentration tend to increase and decrease, respectively, as the selenization temperature increases. Note that the electrical properties of CIGS films are dominated by native defects resulting from deviations from stoichiometric composition, such as vacancies and interstitials [30]. Considering the SEM images presented in Figure 4, increasing selenization temperature results in the improvement of crystallinity and therefore in a decreased total number of defects, which may be related to net carrier concentrations of CIGS films.

4. Conclusions

A two-stage method has been developed to prepare Cu(In, Ga)Se_2 films using Se-containing precursors in Se-vapor selenization process. The effects of precursor composition and selenization temperature on the film properties were investigated. The [Cu]/[In + Ga] and [Ga]/[In + Ga] ratios in CIGS films could be controlled by adjusting the sputtering parameters of the $Cu_{0.8}Ga_{0.2}$ and In_2Se_3 targets. Two sets of films, Cu-poor and Cu-rich films, were intentionally prepared for comparison. It is revealed that the amount of Cu in the precursor films strongly influences the morphology, structural and electrical properties of the subsequent selenized films. XRD analysis shows that Cu(In,Ga)Se_2 solid solution needs higher selenization temperature due to the inclusion of gallium. For Cu-rich films, $Cu_{2-x}Se$ segregation is always

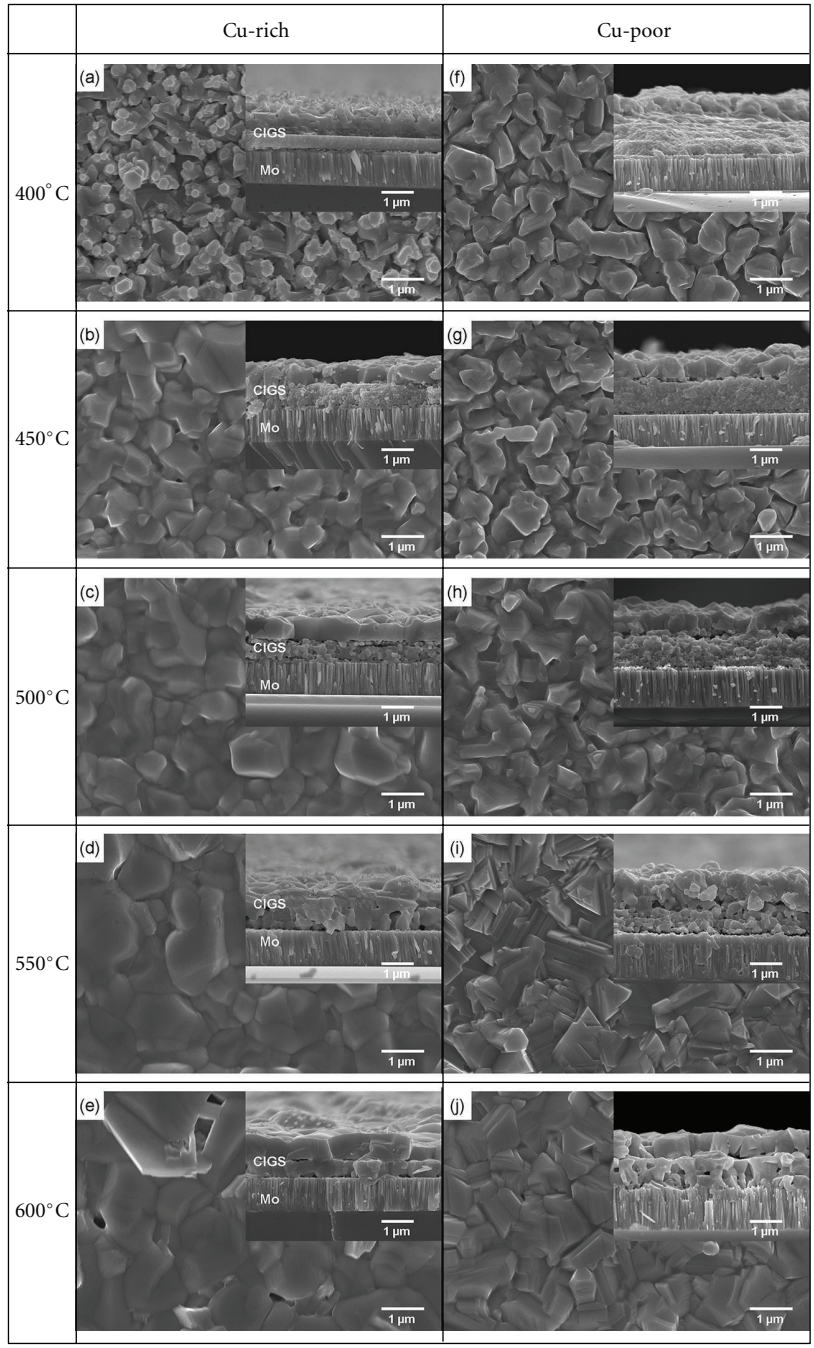

Figure 4: Comparison of surface and cross-section (insets) SEM images of CIGS films selenized from Cu-rich precursor films (left column) and Cu-poor precursor films (right column) at different selenization temperatures: (a), (f) 400°C; (b), (g) 450°C; (c); (h) 500°C, (d), (i) 550°C; (e), (j) 600°C.

present, but for Cu-rich films, it exists only when the selenization temperature was 400°C due to inadequate reaction. In comparison with the Cu-poor films, the Cu-rich films have a higher crystallinity due to the presence of low-temperature liquid Cu-Se phase. The crystallinity of the films improves noticeably as the selenization temperature increases. The resistivity of the Cu-rich films is about three orders of magnitude lower than that of the Cu-poor films, which is attributed to the presence of p-type highly conductive $Cu_{2-x}Se$ phase. In both cases of the Cu-rich and Cu-poor films, the dependence of resistivity on selenization temperature is similar and may be due to the change in film crystallinity and native defects.

Acknowledgments

The authors are thankful to Song Jun for equipment maintenance, Li Jun for XRF measurement, and Chen Feng-en

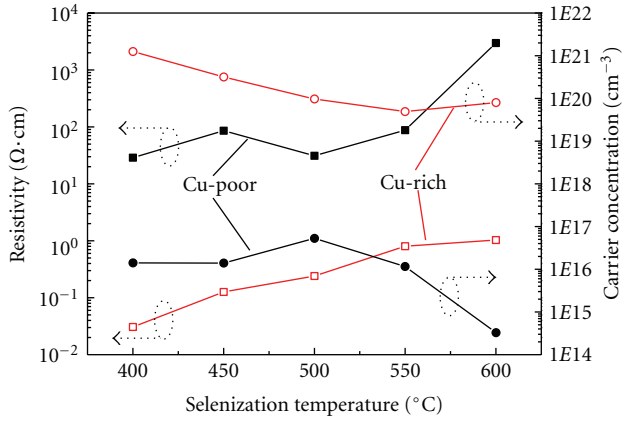

FIGURE 5: Resistivity (squares) and carrier concentration (circles) of CIGS films as a function of selenization temperature. Full and open symbols correspond to CIGS films selenized from Cu-poor precursor films and Cu-rich precursor films, respectively.

for measurement of Raman spectra. This work was financially supported by Initiative Scientific Research Project of Tsinghua University.

References

[1] M. A. Contreras, B. Egaas, K. Ramanathan et al., "Progress toward 20% efficiency in Cu(In,Ga)Se_2 polycrystalline thin-film solar cells," *Progress in Photovoltaics*, vol. 7, no. 4, pp. 311–316, 1999.

[2] P. Jackson, D. Hariskos, and E. Lotter, "New world record efficiency for Cu(In,Ga)Se_2 thin-film solar cells beyond 20%," *Progress in Photovoltaics*, vol. 19, no. 7, pp. 894–897, 2011.

[3] A. Jager-Waldau, "Progress in chalcopyrite compound semiconductor research for photovoltaic applications and transfer of results into actual solar cell production," *Solar Energy Materials and Solar Cells*, vol. 95, no. 6, pp. 1509–1517, 2011.

[4] M. Kaelin, D. Rudmann, and A. N. Tiwari, "Low cost processing of CIGS thin film solar cells," *Solar Energy*, vol. 77, no. 6, pp. 749–756, 2004.

[5] S. Niki, M. Contreras, I. Repins et al., "CIGS absorbers and processes," *Progress in Photovoltaics*, vol. 18, no. 6, pp. 453–466, 2010.

[6] A. Rao, S. Krishnan, G. Sanjeev, K. Siddappa, H. S. Ullal, and X. Z. Wu, "8 MeV electron irradiation studies on electrical characteristics of Cu(In,Ga)Se_2 solar cells," *Solar Energy Materials and Solar Cells*, vol. 93, no. 9, pp. 1618–1623, 2009.

[7] M. A. Green, K. Emery, Y. Hishikawa, and W. Warta, "Solar cell efficiency tables (version 37)," *Progress in Photovoltaics*, vol. 19, no. 1, pp. 84–92, 2011.

[8] O. Lundberg, J. Lu, A. Rockett, M. Edoff, and L. Stolt, "Diffusion of indium and gallium in Cu(In,Ga)Se_2 thin film solar cells," *Journal of Physics and Chemistry of Solids*, vol. 64, no. 9-10, pp. 1499–1504, 2003.

[9] C. L. Jensen, D. E. Tarrant, J. H. Ermer, and G. A. Pollock, "Role of gallium in $CuInSe_2$ solar cells fabricated by a two-stage method," in *Proceedings of the 23rd IEEE Photovoltaic Specialists Conference*, pp. 577–580, Louisville, Ky, USA, May 1993.

[10] U. Rau and H. W. Schock, "Cu(In,Ga)Se_2 thin-film solar cells," in *Solar Cells: Materials, Manufacture and Operation*, T. Markvart and L. Castaner, Eds., pp. 303–349, Elsevier, Oxford, UK, 2005.

[11] J. R. Tuttle, M. Contreras, A. Tennant, D. Albin, and R. Noufi, "High efficiency thin-film Cu (In, Ga) Se_2-based photovoltaic devices: progress towards a universal approach to absorber fabrication," in *Proceedings of the 23rd IEEE Photovoltaic Specialists Conference*, pp. 415–421, Louisville, Ky, USA, May 1993.

[12] M. Venkatachalam, M. D. Kannan, S. Jayakumar, R. Balasundaraprabhu, and N. Muthukumarasamy, "Effect of annealing on the structural properties of electron beam deposited CIGS thin films," *Thin Solid Films*, vol. 516, no. 20, pp. 6848–6852, 2008.

[13] P. Jackson, R. Würz, U. Rau et al., "High quality baseline for high efficiency, Cu(In_{1-x},Ga_x)Se_2 solar cells," *Progress in Photovoltaics*, vol. 15, no. 6, pp. 507–519, 2007.

[14] K. Ramanathan, G. Teeter, J. C. Keane, and R. Noufi, "Properties of high-efficiency $CuInGaSe_2$ thin film solar cells," *Thin Solid Films*, vol. 480-481, pp. 499–502, 2005.

[15] M. A. Contreras, K. Ramanathan, J. AbuShama et al., "Diode characteristics in state-of-the-art ZnO/CdS/ Cu($In_{1-x}Ga_x$)Se_2 solar cells," *Progress in Photovoltaics*, vol. 13, no. 3, pp. 209–216, 2005.

[16] V. F. Gremenok, E. P. Zaretskaya, V. B. Zalesski et al., "Preparation of Cu(In,Ga)Se_2 thin film solar cells by two-stage selenization processes using N_2 gas," *Solar Energy Materials and Solar Cells*, vol. 89, no. 2-3, pp. 129–137, 2005.

[17] J. H. Shi, Z. Q. Li, D. W. Zhang, Q. Q. Liu, Z. Z. Sun, and S. M. Huang, "Fabrication of Cu(In, Ga)Se_2 thin films by sputtering from a single quaternary chalcogenide target," *Progress in Photovoltaics*, vol. 19, no. 2, pp. 160–164, 2011.

[18] V. Alberts, S. Zweigart, and H. W. Schock, "Preparation of device quality $CuInSe_2$ by selenization of Se-containing precursors in H_2Se atmosphere," *Semiconductor Science and Technology*, vol. 12, no. 2, pp. 217–223, 1997.

[19] W. Witte, R. Kniese, and M. Powalla, "Raman investigations of Cu(In,Ga)Se_2 thin films with various copper contents," *Thin Solid Films*, vol. 517, no. 2, pp. 867–869, 2008.

[20] N. Barreau, J. Lähnemann, F. Couzinié-Devy, L. Assmann, P. Bertoncini, and J. Kessler, "Impact of Cu-rich growth on the $CuIn_{1-x}Ga_xSe_2$ surface morphology and related solar cells behaviour," *Solar Energy Materials and Solar Cells*, vol. 93, no. 11, pp. 2013–2019, 2009.

[21] W. Li, Y. Sun, Y. Wang, H. Cai, F. Liu, and Q. He, "Effects of substrate temperature on the properties of facing-target sputtered Al-doped ZnO films," *Solar Energy Materials and Solar Cells*, vol. 91, no. 8, pp. 659–663, 2007.

[22] A. A. Kadam and N. G. Dhere, "Highly efficient $CuIn_{1-x}Ga_xSe_{2-y}S_y$/CdS thin-film solar cells by using diethylselenide as selenium precursor," *Solar Energy Materials and Solar Cells*, vol. 94, no. 5, pp. 738–743, 2010.

[23] R. Caballero and C. Guillén, "Comparative studies between Cu-Ga-Se and Cu-In-Se thin film systems," *Thin Solid Films*, vol. 403-404, pp. 107–111, 2002.

[24] W. Witte, R. Kniese, A. Eicke, and M. Powalla, "Influence of the GA content on the Mo/Cu(In,Ga)Se_2 interface formation," in *Proceedings of the 4th IEEE World Conference on Photovoltaic Energy Conversion*, vol. 1, pp. 553–556, May 2006.

[25] T. Delsol, A. P. Samantilleke, N. B. Chaure, P. H. Gardiner, M. Simmonds, and I. M. Dharmadasa, "Experimental study of graded bandgap Cu(InGa)$(SeS)_2$ thin films grown on glass/molybdenum substrates by selenization and sulphidation," *Solar Energy Materials and Solar Cells*, vol. 82, no. 4, pp. 587–599, 2004.

[26] E. P. Zaretskaya, V. F. Gremenok, V. Riede et al., "Raman spectroscopy of $CuInSe_2$ thin films prepared by selenization," *Journal of Physics and Chemistry of Solids*, vol. 64, no. 9-10, pp. 1989–1993, 2003.

[27] B. J. Stanbery, "Copper indium selenides and related materials for photovoltaic devices," *Critical Reviews in Solid State and Materials Sciences*, vol. 27, no. 2, pp. 73–117, 2002.

[28] R. Klenk, T. Walter, H. W. Schock, and D. Cahen, "A model for the successful growth of polycrystalline films of $CuInSe_2$ by multisource physical vacuum evaporation," *Advanced Materials*, vol. 5, no. 2, pp. 114–119, 1993.

[29] Y. Goushi, H. Hakuma, K. Tabuchi, S. Kijima, and K. Kushiya, "Fabrication of pentanary $Cu(InGa)(SeS)_2$ absorbers by selenization and sulfurization," *Solar Energy Materials and Solar Cells*, vol. 93, no. 8, pp. 1318–1320, 2009.

[30] R. Noufi, R. Axton, C. Herrington, and S. K. Deb, "Electronic properties versus composition of thin films of $CuInSe_2$," *Applied Physics Letters*, vol. 45, no. 6, pp. 668–670, 1984.